http://dx.doi.org/10.5012/bkcs.2012.33.10.3213

Ni/ZnO-based Adsorbents Supported on Al_2O_3, SiO_2, TiO_2, ZrO_2: A Comparison for Desulfurization of Model Gasoline by Reactive Adsorption

Xuan Meng, Huan Huang, Huixin Weng, and Li Shi*

The State Key Laboratory of Chemical Engineering, East China University of Science and Technology, Shanghai 200237, China
**E-mail: yyshi@ecust.edu.cn*
Received April 13, 2012, Accepted July 4, 2012

Reactive adsorption desulfurization (RADS) experiments were conducted over a series of commercial metal oxide supports (Al_2O_3-, SiO_2-, TiO_2- and ZrO_2-) supported Ni/ZnO adsorbents. The adsorbents were characterized by X-ray diffraction (XRD), temperature programmed reduction (TPR), and Fourier transform infrared spectroscopy (FTIR) in order to find out the influence of specific types of surface chemistry and structural characteristics on the sulfur adsorptive capacity. The desulfurization performance of all the studied adsorbents decreased in the following order: Ni/ZnO-TiO_2 > Ni/ZnO-ZrO_2 > Ni/ZnO-SiO_2 > Ni/ZnO-Al_2O_3. Ni/ZnO-TiO_2 shows the best performance and the three hour sulfur capacity can achieve 12.34 mg S/g adsorbent with a WHSV of 4 h^{-1}. Various characterization techniques suggest that weak interaction between active component and support component, high dispersion of NiO and ZnO, high reducibility and large total Lewis acidity of the adsorbents are important factors in achieving better RADS performance.

Key Words : Reactive adsorption desulfurization, Thiophene, Ni/ZnO, Metal oxide support

Introduction

Due to the stringent fuel specifications for the transportation fuel and the severe requirement of liquid hydrocarbon fuels for fuel cell applications, effective processes for deep desulfurization of transportation fuels, such as diesel, gasoline, and jet fuel, have attracted more and more attention.[1] The conventional hydrodesulfurization (HDS) is a typical and very effective desulfurization process. However, to produce ultra-low-sulfur gasoline to meet the requirement of new regulations or fuel cell applications, the reactor size of HDS process needs to be 5-15 times increased in comparison with those currently used.[2] Furthermore, loss of olefin may be significant because of the conversion of olefin to paraffin during the desulfurization process.

Several non-HDS-based desulfurization technologies such as adsorptive desulfurization,[3,4] oxidative desulfurization,[5,6] extraction using ionic liquids,[7,8] biocatalytic treatment,[9] *etc.*, have been proposed recently for the desulfurization of liquid fuels. Among them, the reactive adsorption desulfurization (RADS) is considered to be one of the most promising approaches for deep desulfurization because it combines the advantages of both the catalytic HDS and adsorption.[10,11] The S-Zorb process of Conoco Philips Petroleum Co. based on RADS at elevated temperatures under a low H_2 pressure has been proved to be effective for the production of low-sulfur gasoline and diesel fuel.[12] Several accounts have been published on fuel desulfurization by Ni/ZnO adsorbents based on the mechanism of RADS after Tawara *et al.*[10] reported that Ni/ZnO could be used as an "adsorptive HDS catalyst". Babich and Moulijn[13] described an overall reaction mechanism on the basis of the data of Tawara *et al.* Bezverkhyy *et al.*[14,15] studied the kinetics of thiophene reactive adsorption on Ni/ZnO by thermal gravimetric analysis and suggested some features of the reaction mechanism. Huang *et al.*[16] investigated the transfer of sulfur species in the RADS process by the sulfur K-edge X-ray absorption near-edge structure (XANES) and XRD and confirmed that the organic sulfur compounds are first decomposed on surface of Ni/ZnO to form Ni_3S_2, followed by the reduction of Ni_3S_2 to form H_2S and stored in the adsorbent accompanied by the conversion of ZnO into ZnS.

Mixed oxides have drawn much attention that could improve textural properties, enhance activity, improve active metal dispersion, eliminate or reduce coke formation, and prevent thermal sintering when used as a support material.[17] Gao *et al.*[18] studied the RADS experiments of FCC gasoline over a Ni/ZnO-SiO_2-Al_2O_3 adsorbent and confirmed that the presence of SiO_2 and Al_2O_3 can improve the desulfurization performance of FCC gasoline and reduce the RON loss under the optimal operating conditions. Sasaoka *et al.*[19] studied a high-temperature desulfurization adsorbent by add 5 or 10 mol % ZrO_2 to 50 mol % ZnO-50 mol % TiO_2. They found that the addition of ZrO_2 greatly improved the reactivity for H_2S removal and its regenerability. However, few efforts have been made to compare the reactive adsorption desulfurization performance for Ni/ZnO deposited on various metal oxide supports under the same condition.

In the present study, a series of commercial metal oxide supports (Al_2O_3-, SiO_2-, TiO_2- and ZrO_2-) supported Ni/ZnO adsorbents were prepared and used on the RADS experiments. The main objective of this work is to compare the performance of different metal oxide supported Ni/ZnO adsorbents for RADS and to understand the specific types of surface chemistry and structural characteristics responsible for the adsorptive capacity.

Experimental Section

Feedstocks and Adsorbents. In this study, a model gasoline was prepared by adding thiophene (analytical grade from Aldrich) to sulfur-free *n*-octane (analytical grade from Sinopharm Chemical Reagent Co., Ltd.) with the sulfur concentration of 2000 ppmw.

Supported Ni/ZnO-based adsorbents used in this study were prepared by kneading method.[20] ZnO and Ni_2O_3 were sufficiently mixed with an inorganic binder, then γ-Al_2O_3, SiO_2, TiO_2, ZrO_2 were added separately to the mixture in order to achieve the desirable reactivity and attrition resistance (all chemicals were purchased from Sinopharm Chemical Reagent Co., Ltd.). Next, a liquid binder, dilute nitric acid, was added to the mixture to make the slurry. An extruder was used to formulate pellets to an outer diameter of 1 mm from the slurry. All of the adsorbents were dried overnight to remove moisture at 120 ºC in an oven and then calcined in air at 600 ºC for 1 h in a muffle furnace. The pellets were crushed and sieved to 20-40 mesh to use. Compositions of Ni/ZnO-based adsorbents are shown in Table 1.

Characterization of Adsorbents.

X-ray Diffraction: An X-ray diffraction (XRD) technique was used to characterize the crystal structure. In this work, XRD patterns were obtained with a Siemens D-500 X-ray diffractometer equipped with Ni-filtrated Cu Kα radiation (40 kV, 100 mA). The 2θ scanning angle range was 10-80º with a step of 0.02 deg/s.

Acidity Characterization: The amount of acid, the acid density, and the acid variety were measured *via* FTIR spectroscopy (Magna-IR550, Nicolet Company), using pyridine as the probe molecule. There are two varieties of acid: one is a Brønsted acid (denoted as B), whose characteristic absorption peak is observed at 1540 cm^{-1}, and the other is a Lewis acid (denoted as L), whose characteristic absorption peak is located at 1450 cm^{-1}. The pyridine adsorption, which gives measured after desorption at 200 ºC, is the total acid sites (T). The quantification method for Lewis acidic site and Brønsted acidic site was based on Lambert-Beer law: $A = \xi \cdot C \cdot d$, where A is absorbance, C is sample concentration, ξ is extinction coefficient and d is sample thickness. The surface acid contents of adsorbents for Lewis acid and Brønsted acid were calculated by using empirical formulas which are obtained from the relevant experiments.

$$C_L\ (\text{mol}\cdot\text{g}^{-1}) = 3.73 \times 10^{-4} \cdot A_L \quad (1)$$

$$C_B\ (\text{mol}\cdot\text{g}^{-1}) = 9.90 \times 10^{-4} \cdot A_B \quad (2)$$

Table 1. Compositions of Ni/ZnO-based adsorbents

Sample	Zn/Ni (mole ratio)	Support
Ni/ZnO-Al_2O_3	0.4	γ-Al_2O_3 (50 wt %)
Ni/ZnO-TiO_2	0.4	TiO_2 (50 wt %)
Ni/ZnO-ZrO_2	0.4	ZrO_2 (50 wt %)
Ni/ZnO-SiO_2	0.4	SiO_2 (50 wt %)

where C_L and C_B are respectively Lewis acid contents and Brønsted acid contents ($\text{mol}\cdot\text{g}^{-1}$), A_L and A_B are respectively peak areas in 1450 cm^{-1} (denoted as L) and in 1540 cm^{-1} (denoted as B).

Temperature Programmed Reduction (TPR): TPR experiments were performed to determine the reducibility of the surface oxides. Prior to the TPR experiments, the samples were pretreated in a He flow up to 250 °C and kept for 1 h to remove the adsorbed water and other contaminants followed by cooling to 25 °C. The reducing gas containing 5% H_2 balanced with Ar mixture was passed over the samples at a flow rate of 30 mL/min with the heating rate of 10 °C/min up to 800 °C and kept at that temperature for 20 min.

Adsorption Experiment. The RADS experiments were performed at 400 °C under the pressure of 1.0 MPa with a pure H_2 flow (40 mL/min). About 1.0 g of the adsorbent was used in a stainless steel column having a bed dimension of 6 mm i.d. and 250 mm length. The packed column was placed in a multi-channel convection oven designed in our laboratory for the adsorption experiments. In order to ensure that the Ni in the Ni/ZnO-based adsorbent is in the reduced form, the adsorbent bed was pretreated with H_2 gas at a flow rate of 30 mL/min under 0.5 MPa at 450 °C, and kept at this temperature for about 1 h. After the pretreatment, the oven temperature and pressure was increased to the desired adsorption temperature and pressure in the H_2 stream. In the adsorption experiments, the model fuel was sent into the adsorbent column by a micro-injection pump, flowed down through the adsorbent bed at a weight hourly space velocity (WHSV) of 4 h^{-1}, H_2/oil volume ratio of 400. The liquid products were collected in a cryogenic trap with ice water bath and subjected to analysis periodically. The treated-fuel samples were analyzed, quantitatively using a Agilent 6890A Gas Chromatograph and qualitatively using a Finnigan SSQ710 GC-MS. The distributions of sulfur compounds in the products were analyzed in the Agilent 6890A Gas Chromatograph coupled with a flame photometric detector (FPD). The thiohene conversion (x) and sulfur capacity (a) were calculated based on the GC results. They were calculated according to:

$$x(\%) = \frac{C_0 - C}{C_0} \times 100 \quad (3)$$

$$a(\text{mgS/g sorbent}) = (C_0 - C) \times S \times t \times 1000 \quad (4)$$

where C_0 is the initial sulfur concentration (g/g), C is the final sulfur concentration (g/g), S is the weight hourly space velocity (h^{-1}) and t is the liquid flow time (h).

Results and Discussion

XRD Characterizations. X-ray diffraction analysis in Figure 1 was carried out to identify the mineralogical structure of Ni/ZnO-based adsorbents supported by Al_2O_3, SiO_2, TiO_2 and ZrO_2 respectively. XRD pattern of Ni/ZnO-Al_2O_3

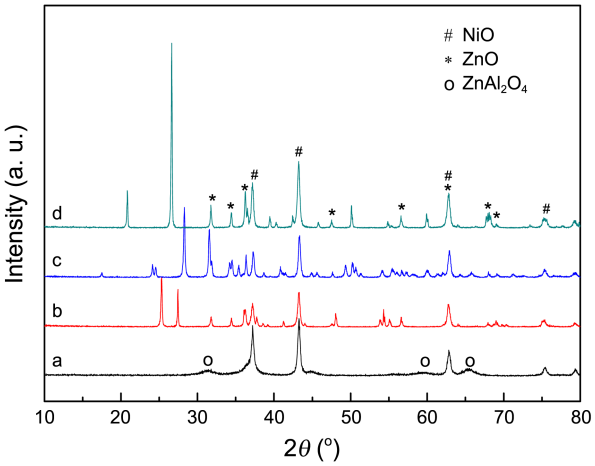

Figure 1. X-ray diffraction (XRD) patterns of samples. (a) Ni/ZnO-Al_2O_3 (b) Ni/ZnO-TiO_2 (c) Ni/ZnO-ZrO_2 (d) Ni/ZnO-SiO_2.

(Figure 1(a)) displays the strong characteristic reflections for cubic crystalline NiO at 2θ of 37.22°, 43.26°, 62.84°, 75.41°, 79.41° and without any obvious reflection for crystalline ZnO and Al_2O_3. In addition, broad diffraction peaks of $ZnAl_2O_4$ are found at 2θ of 31.24°, 59.35°, 65.24° which indicate that there are strong interactions between ZnO and Al_2O_3.

Furthermore, the anatase (2θ of 25.28°, 37.80°, 48.05°, 53.89°) and rutile (2θ of 27.44°, 36.09°, 41.25°, 54.34°) phase of TiO_2 are both found in the XRD pattern of Ni/ZnO-TiO_2 (Figure 1(b)). The characteristic reflections for crystalline NiO and ZnO in Figure 1(b) show weakest intensities and broadest diffraction bands which means incorporated NiO and ZnO particles have a better dispersion and smaller crystal size on titania supports than the others.

XRD pattern of Ni/ZnO-ZrO_2 (Figure 1(c)) reveals the characteristic reflections for monoclinic phase of ZrO_2 at 2θ of 28.18°, 31.47°, 50.57°, 62.85°. The intensities of diffraction peaks for NiO and ZnO in the Ni/ZnO-ZrO_2 are stronger than those on with Ni/ZnO-TiO_2, implying that NiO and ZnO in the Ni/ZnO-ZrO_2 have higher crystallinity and larger particle size.

Compared to other three adsorbents, XRD pattern of Ni/ZnO-SiO_2 (Figure 1(d)) shows the strongest intensities of diffraction peaks for NiO and ZnO, indicating that the crystallinity of NiO and ZnO in the Ni/ZnO-SiO_2 is highest in the four samples and the particle size is largest. In addition, the characteristic reflections for hexagonal crystalline SiO_2 are observed.

Temperature Programmed Reduction (TPR) Characterizations. The TPR profiles of the samples are presented in Figure 2. All the four samples have an obvious peak with T_{max} at around 370 °C, which can be attributed to the reduction of NiO particles with no interaction with the supports.[21] The micro shoulder peak at about 260-285 °C corresponds to the reduction of Ni_2O_3 according to the literature data,[22] indicating the presence of a small amount of Ni_2O_3, and the amount in Ni/ZnO-Al_2O_3 is bigger than in other three samples. Li *et al.*[23] have reported that Ni species

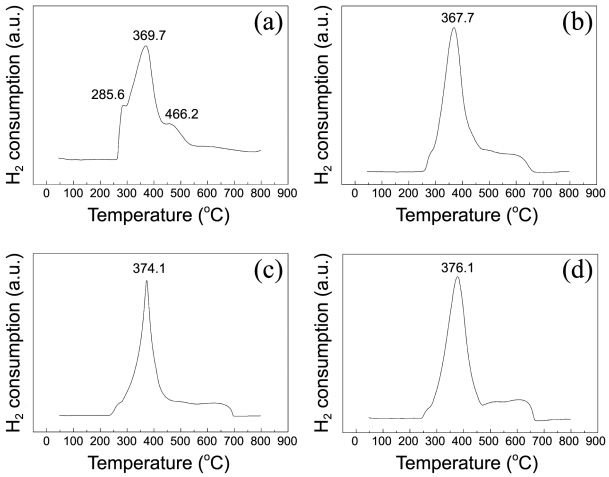

Figure 2. Temperature-programmed reduction (TPR) profiles of samples. (a)Ni/ZnO-Al_2O_3, (b) Ni/ZnO-TiO_2, (c) Ni/ZnO-ZrO_2, (d) Ni/ZnO-SiO_2.

interacting with tetrahedrally coordinated sites of γ-Al_2O_3 is not reducible at temperatures below 400 °C. Therefore, another shoulder peak with T_{max} at around 460 °C in the profile of Ni/ZnO-Al_2O_3 can be assigned to the reduction of Ni (tetra). The broad peak in the four samples (within about 500 °C and 700 °C) could correspond to the reduction of ZnO species on the solid surface which is consistent with the conclusion of Barroso *et al.*[24] and Ruth *et al.*[25] It is observed that the reduction of Ni/ZnO-Al_2O_3 hasn't completed even when the temperature up to 800 °C, which can be related to the spinel species like $ZnAl_2O_4$, and the presence of $ZnAl_2O_4$ is also confirmed by XRD Characterization. The results imply that the formation of spinel species can reduce the reducibility of adsorbent.

Acidity Characterization. Pyridine FTIR spectra for the adsorption of pyridine at 200 °C was used to investigate the type and number of the surface acid sites on the Ni/ZnO-based adsorbents supported by Al_2O_3, SiO_2, TiO_2, ZrO_2 respectively (see Figure 3). The spectra displayed many bands in the wavenumber range of 1400-1560 cm^{-1}, which was attributed to the interaction of pyridine with Lewis (L)

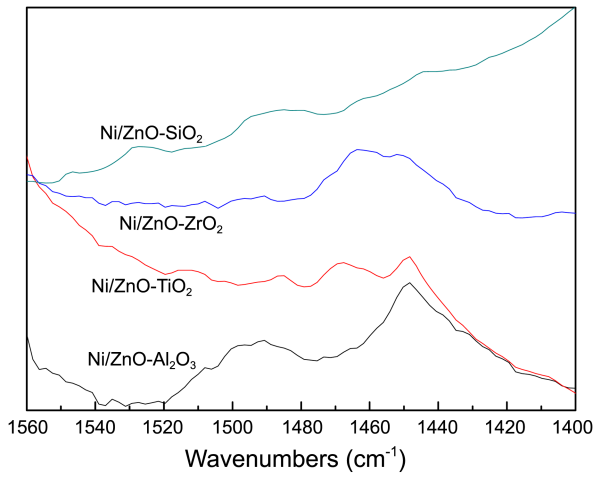

Figure 3. FT-IR spectra of the adsorbents at 200 °C.

Table 2. Surface acid content of adsorbents ($\times 10^{-4}$ mol·g^{-1})

Sample	T	T_L	T_B
Ni/ZnO-Al_2O_3	5.194	5.194	0
Ni/ZnO-TiO_2	5.321	5.321	0
Ni/ZnO-ZrO_2	5.783	5.232	0.551
Ni/ZnO-SiO_2	1.525	0.119	1.406

T: Total acid; T_L: total L acid; T_B: total B acid

and Brønsted (B) acid sites on the sample surfaces. We mainly observed the bands at around 1450 cm^{-1} of Ni/ZnO-Al_2O_3, Ni/ZnO-TiO_2 and Ni/ZnO-ZrO_2, arising due to the 19b ν(C-C) vibration of pyridine adsorbed at the Lewis acid sites. There is almost no band observed at 1540 cm^{-1}, revealing almost no Brønsted acid sites on all the four samples.

The corresponding calculated concentration of acid sites is summarized in Table 2. We can see from Table 2 that the amount of total L acid sites on Ni/ZnO-TiO_2 is more than other three samples. It should be noticed that almost no L acid sites and B acid sites was found on Ni/ZnO-SiO_2, indicating that the physical adsorption is on the dominant position during the adsorption of thiophene on Ni/ZnO-SiO_2.

Adsorptive Performance. The results of RADS of model gasoline at 400 °C and at the weight hourly space velocity (WHSV) of 4 h^{-1} over various supported Ni/ZnO-based adsorbents operating under identical experimental conditions are shown in Figure 4, and the three hour accumulated sulfur capacity of the adsorbents are summarized in Figure 5. As can be seen from Figure 4, the desulfurization performance of all the four samples reduced rapidly at the beginning of the experiment, and met a stabilization while the treated volume of model gasoline increased to about 8 mL/g adsorbent. It should be noted that a thiophene concentration (2000 ppm) much higher than that found in the FCC gasoline (typically in the range of 500 ppm-800 ppm) of industrial refineries was used for these experiments. Among the adsorbents studied, Ni/ZnO-TiO_2 adsorbent showed

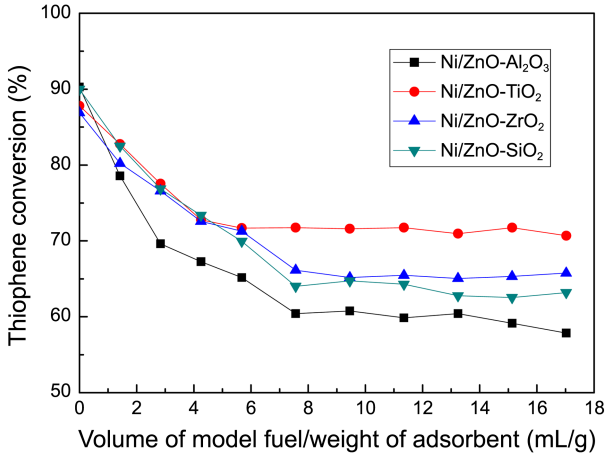

Figure 4. Effect of different metal oxide support on RADS performance (T = 400 °C, P = 1 MPa, WHSV = 4 h^{-1}, H_2/oil = 400).

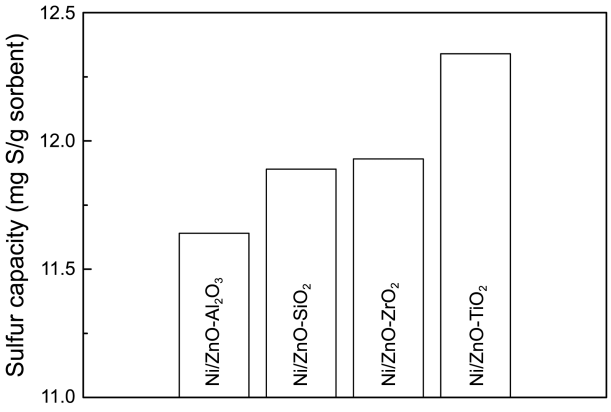

Figure 5. Three hour accumulated sulfur capacity of the adsorbents.

superior adsorptive performance over the others and the three hour sulfur capacity can achieve 12.34 mg S/g adsorbent. The desulfurization performance of all the studied adsorbents decreased in the following order: Ni/ZnO-TiO_2 > Ni/ZnO-ZrO_2 > Ni/ZnO-SiO_2 > Ni/ZnO-Al_2O_3. As represented in XRD characterization, there is no obvious reflection for crystalline ZnO and Al_2O_3 in the sample NiZnO/Al_2O_3, while broad diffraction peaks of $ZnAl_2O_4$ are found, it indicates that there are strong interactions between ZnO and Al_2O_3. Tawara *et al.*[10] reported that Ni/ZnO is an auto-regenerative adsorptive UD-HDS catalyst, the ZnO support is regarded to regenerate sulfur-poisoned surface Ni to active surface Ni by accepting H_2S. In the reactive adsorption desulfurization system, ZnO is considered to the active component, while $ZnAl_2O_4$ belongs to the non-active component. So the formation of $ZnAl_2O_4$ in the sample NiZnO/Al_2O_3 may be the reason for lower activity. For the other three support adsorbents, the diffraction peaks of ZnO could be all detected in the XRD patterns without a spinel structure. This indicates that the interactions between ZnO component and the support components in the Ni/ZnO-TiO_2,Ni/ZnO-ZrO_2 and Ni/ZnO-SiO_2 samples are weaker than that in the NiZnO/Al_2O_3 sample. Comparison of the three support adsorbents, NiO and ZnO particles have a best dispersion on titania support, which makes the number of active centers on Ni/ZnO-TiO_2 adsorbent more than the other three adsorbents, and contribute to a better adsorptive performance. In view of this point, a relatively weak interaction between the ZnO component and the support component in the Ni/ZnO-adsorbents might play a very important role in accelerating the transformation rate of NiS to ZnS. Both XRD and TPR results reveal the presence of strong interactions between ZnO and Al_2O_3, which significantly reduce the reducibility and contribute to a low desulfurization activity of Ni/ZnO-Al_2O_3. It is reported that thiophenic compounds with lone pair electrons present Lewis basicity which is apt to adsorb on the Lewis acid site.[26] The results of FT-IR spectra, the amount of total L acid suites on Ni/ZnO-TiO_2 is more than other three samples, also gives a demonstration to the above conclusion. Although Ni/ZnO-SiO_2 possesses the fewest amount of total L acid

sites, the performance of Ni/ZnO-SiO_2 is better than that of the Ni/ZnO-Al_2O_3 sample due to the weak interaction between active component and support component according to the results of XRD and TPR respectively.

Conclusion

The physical characteristics and surface chemical properties of the adsorbents are significantly related to the metal oxides which are incorporated with Ni/ZnO. In conclusion, all characterization results proved that weak interaction between active component and support component, high dispersion of NiO and ZnO, high reducibility and large total Lewis acidity of the adsorbents are important factors in achieving better RADS performance. The formation of spinel species can reduce the reducibility of adsorbents and lead to a low activity for the adsorption of thiophene. Among the Al_2O_3-, TiO_2-, ZrO_2-, and SiO_2-supported Ni/ZnO adsorbents studied for the RADS of model gasoline, Ni/ZnO-TiO_2 showed the best performance and the three hour sulfur capacity can achieve 12.34 mg S/g adsorbent with a WHSV of 4 h^{-1}.

References

1. Sentorun-Shalaby, C.; Saha, S. K.; Ma, X. L.; Song, C. S. *Appl. Catal. B: Environmental* **2011**, *101*, 718.
2. Hernández-Maldonado, A. J.; Yang, R. T. *J. Am. Chem. Soc.* **2004**, *126*, 992.
3. Yang, R. T.; Hernández-Maldonado, A. J.; Cannella, W. *Science* **2003**, *301*, 79.
4. Song, C. S.; Ma, X. L. *Appl. Catal. B: Environmental* **2003**, *41*, 207.
5. Lü, H. Y.; Gao, J. B.; Jiang, Z. X.; Jing, F.; Yang, Y. X.; Wang, G.; Li, C. *J. Catal.* **2006**, *239*, 369.
6. Huleaa, V.; Fajulaa, F.; Bousquet, J. *J. Catal.* **2001**, *198*, 179.
7. Bösmann, A.; Datsevich, L.; Jess, A.; Lauter, A.; Schmitz, C.; Wasserscheid, P. *Chem. Commun.* **2001**, 2494.
8. Jochen, E.; Peter, W.; Andreas, J. *Green Chem.* **2004**, *6*, 316.
9. Gray, K. A.; Pogrebinsky, O. S.; Mrachlko, G. T.; Xi, L.; Monticello, D. J.; Squires, C. H. *Nat. Biotechnol.* **1996**, *14*, 1705.
10. Tawara, K.; Nishimura, T.; Iwanami, H. *Sekiyu Gakkaishi.* **2000**, *43*, 114.
11. Tawara, K.; Nishimura, T.; Iwanami, H.; Nishimoto, T.; Hasuike, T. *Sekiyu Gakkaishi.* **2001**, *44*, 43.
12. Tang, H.; Li, Q.; Song, Z. Y.; Li, W. L.; Xing, J. M. *Catal. Commun.* **2011**, *12*, 1079.
13. Babich, I. V.; Moulijin, J. A. *Fuel* **2003**, *82*, 607.
14. Bezverkhyy, I.; Ryzhikov, A.; Gadacz, G.; Bellat J. P. *Catal. Today* **2008**, *130*, 199.
15. Ryzhikov, A.; Bezverkhyy, I.; Bellat, J. P. *Appl. Catal. B: Environmental* **2008**, *84*, 766.
16. Huang, L. C.; Wang, G. F.; Qin, Z. F.; Du, M. X.; Dong, M.; Ge, H.; Wu, Z. W.; Zhao, Y. D.; Ma, C. Y.; Hu, T. D.; Wang, J. G. *Catal. Commun.* **2010**, *11*, 592.
17. Hussam, H. I.; Raphael, O. I. *Energy & Fuels* **2008**, *22*, 878.
18. Fan, J. X.; Wang, G.; Sun, Y.; Xu, C. M.; Zhou, H. J.; Zhou, G. L.; Gao, J. S. *Ind. Eng. Chem. Res.* **2010**, *49*, 8450.
19. Sasaoka, E.; Sada, N. *Ind. Eng. Chem. Res.* **1999**, *38*, 958.
20. Tang, X. L.; Shi, L. *Langmuir* **2011**, *27*, 11999.
21. Li, J.; Tian, W. P.; Shi, L. *Ind. Eng. Chem. Res.* **2010**, *49*, 11837.
22. Ho, S. C.; Chou, T. C. *Ind. Eng. Chem. Res.* **1996**, *34*, 2279.
23. Li, C. P.; Chen, Y. W. *Thermochim. Acta* **1995**, *256*, 457.
24. Barroso, M. N.; Gomez, M. F.; Arrúa, L. A.; Abello, M. C. *Appl. Catal. A: General* **2006**, *304*, 116.
25. Álvarez, R.; Tóffolo, A.; Pérez, V.; Linares, C. F. *Catal. Lett.* **2010**, *137*, 150.
26. Larrubia, M. A.; Ramirez, J.; Busca, G. A. *Applied Catalysis A: General* **2002**, *224*, 167.